Effect of Beam Broadening in Directional Beamforming-Based Cellular Networks

Gosan Noh

Dept. of Electronic Engineering, Hanbat National University, Daejeon 34158, Korea
E-mail: gsnoh@hanbat.ac.kr

Abstract—The use of directional beamforming at a base station equipped with a linear antenna array has the potential to significantly increase the spectrum utilization efficiency of a cellular network by focusing the information-bearing signal only to the direction of a target mobile user. Unfortunately, however, this beamforming gain can be reduced by the beam broadening effect which broadens the beam width and reduces the directivity gain when the beam is steered away from the boresight direction. Hence, in this paper, assuming poisson point process (PPP)-distributed base stations, we analyze the coverage probability of a directional beamforming-based cellular network considering the beam broadening effect. Analyses are done with the general Nakagami-m fading channel, including two special cases: Rayleigh fading ($m = 1$) and static ($m \to \infty$) channels. Numerical results show that, although the beam broadening effect can lead to some coverage loss, the achieved gain by the directional beamforming is still significant.

Index Terms—Beamforming, fading, stochastic geometry.

I. Introduction

In order to cope with wireless traffic explosion, 5G networks are required to support multi-Gbps data rate [1], which can be achieved by advanced multi-antenna techniques such as massive multiple-input-multiple-output (MIMO). Using such a massive number of antennas, beamforming with a high directivity gain and a narrow beam width is achievable, and the beam direction can be easily steered by controlling the phase and amplitude of each antenna element [2]. By doing so, only mobile users in the direction of the steered beam are subject to reception of the intended signal, achieving much higher spatial frequency reuse.

One concern when employing directional beamforming is the phenomenon of so-called *beam broadening* [3], [4]. As the beam is steered away from the boresight direction, the beam width broadens and the directivity gain decreases. The reason of beam broadening is the reduced effective aperture size [3], [5]. This beam broadening effect should be considered when deploying the directional beamforming-based cellular network.

Another consideration is randomized base station locations, originating from dense deployment of small cells such as picocells and femtocells for achieving high spatial reuse. These small cells are usually deployed in an unplanned manner, and their locations will be highly irregular [6]. Hence, stochastic geometry approach is more effective than traditional hexagonal grid model in analyzing the performance of such highly dense and randomly located cellular networks from conventional sub-6GHz to mmWave bands [7], [8]. Poisson point process (PPP)-based base station location modeling allows a tractable analytic model for coverage probability evaluation [7].

Hence, in this paper, we investigate whether and how much directional beamforming is effective for improving cellular network performance under the aforementioned practical considerations of beam broadening effects and random base station locations. We derive a general expression for the coverage probability that a mobile user can achieve in the downlink of a directional beamforming-based cellular network under a Nakagami-m fading channel assumption. More simplified single-integral and asymptotic closed-form expressions are also obtained when each link approaches Rayleigh fading ($m = 1$) or static ($m \to \infty$) channel.

II. System Model

Consider a downlink cellular network consisting of base stations distributed according to a homogeneous PPP Φ with intensity λ in a two-dimensional Euclidean plane $\mathbb{R}^2$. Mobile users are distributed as a stationary point process independent of the base stations. Throughout the analysis, we focus on a typical mobile user located at the origin o using the Slivnyak's theorem [7]. We assume that each mobile user is associated with the closest base station, forming a Voronoi tessellation on the plane. We also assume an orthogonal multiple access technique, so that there is no intra-cell interference.

Employing linear antenna array at base stations, directional beamforming in the horizontal direction is supported, i.e., a mobile user at a specific location is served by a beam uniquely steered to it while rarely interfered by the beams for other users. We assume each mobile user has an omnidirectional single antenna due to limited power and dimension.

For modeling the antenna pattern of the antenna array at the base station, we employ a rectangular mask model for spatial filtering taken from the 3GPP 5G channel model [9]. Assuming the boresight direction of $\phi = 0°$, the antenna array pattern can be represented as

$$F(\phi, \phi_{\mathrm{BW}}) = \begin{cases} G, & |\phi| \leq \phi_{\mathrm{BW}}/2 \\ 0, & \text{otherwise,} \end{cases} \tag{1}$$

where G is a directivity gain and ϕ_{BW} is a beam width.

It is not possible to cover all azimuthal directions due to physical limitations of a linear array, i.e., steering beam larger than $90°$ is not possible. Hence, we employ sectorization at

each base station, i.e., each cell is divided into K sectors. The antenna array at each sector covers $2\pi/K$ radians.

Another concern when employing the linear antenna array is the beam broadening, which is a phenomenon that the beam width broadens (at the same time the directivity gain decreases) when steered away from the boresight direction. The reason of beam broadening is due to the reduced effective aperture size [3]. With the steered angle θ, the beam width and the directivity gain become [3]:

$$\tilde{\phi}_{\text{BW}}(\theta) \approx \frac{\phi_{\text{BW}}}{\cos\theta} \quad \text{and} \quad \tilde{G}(\theta) \approx G\cos\theta. \tag{2}$$

A standard path loss model is used with a path loss exponent α. For short-term fading, Nakagami-m fading distribution is employed, which well characterizes both the LOS and NLOS components and includes two special cases: NLOS-dominant Rayleigh fading ($m = 1$) and LOS-dominant static ($m \to \infty$) channels. The corresponding channel power gains will be Gamma distributed with the probability density function (PDF) of $f_x(x) = \frac{m^m}{\Gamma(m)}x^{m-1}e^{-mx}$ [10]. We denote the channel power gain of a desired mobile user as h and the base station transmit power as P. Then, the resulting signal-to-interference-plus-noise ratio (SINR) at the typical mobile user with a distance r from its tagged base station (b_0) is given by

$$\text{SINR} = \frac{GPhr^{-\alpha}\cos\theta}{I_r + N_0}, \tag{3}$$

where $I_r = \sum_{i \in \Phi \setminus b_0} GPg_i l_i^{-a}\cos\psi_i$. We denote g_i, l_i, and ψ_i as channel power gain, distance, and steered angle from the i-th interferer base station, respectively. N_0 is noise power.

III. Coverage Analysis

A. Effective Base Station Density

Each interferer base station creates a directional beam only within its beam width. So we define Φ_{eff} as a set of interferer base stations effectively interfering the typical mobile user.

By thinning theorem [11], Φ_{eff} is a PPP with density λ_{eff} proportional to the ratio of the beam width to the entire direction. Since the mobile users are PPP distributed, the beam steering angle θ follows the uniform distribution over the interval $[-\frac{\pi}{K}, \frac{\pi}{K}]$.

Averaging over the angle θ, λ_{eff} can be calculated as [12]:

$$\lambda_{\text{eff}} = \mathbb{E}\left[\frac{\phi_{\text{BW}}}{2\pi\cos\theta}\lambda\right] = \frac{\phi_{\text{BW}}}{2\pi}\int_{-\frac{\pi}{K}}^{\frac{\pi}{K}}\frac{1}{\cos\theta}\frac{K}{2\pi}\text{d}\theta \cdot \lambda$$

$$= \underbrace{\frac{\phi_{\text{BW}}K}{\pi^2}\log\left(1 + \frac{2}{\cot\left(\frac{\pi}{2K}\right) - 1}\right)}_{\triangleq\rho:\text{ effective interferer ratio}} \cdot \lambda. \tag{4}$$

B. Coverage Probability Calculation

The coverage probability is defined as the probability that a typical mobile user is in coverage, which can be satisfied if its received SINR exceeds a target threshold T:

$$P_c \triangleq \mathbb{P}[\text{SINR} > T]. \tag{5}$$

Assuming highly dense cellular networks, we consider an interference-limited environment with negligible noise, i.e., $N_0 \to 0$ [7]. This interference-limited assumption is also applicable even to highly dense mmWave networks [11], [13].

We first consider the most general fading case where each link is Nakagami-m faded in the following proposition.

Proposition 1 (Most general case): The coverage probability for a typical mobile user experiencing Nakagami-m fading when directional beamforming is used at the base station is

$$P_c = \lambda K \sum_{k=0}^{m-1}\int_{-\frac{\pi}{K}}^{\frac{\pi}{K}}\int_0^\infty re^{-\pi\lambda r^2}\left[\frac{(-s)^k}{k!}\frac{\text{d}^k}{\text{d}s^k}\mathcal{L}_{I_r}(s)\right]_{s=\frac{mTr^\alpha}{GP\cos\theta}}\text{d}r\text{d}\theta, \tag{6}$$

where

$$\mathcal{L}_{I_r}(s) = \frac{K}{2\pi}e^{\pi\lambda_{\text{eff}}r^2}\int_{-\frac{\pi}{K}}^{\frac{\pi}{K}}\exp\left(-\frac{\pi\lambda_{\text{eff}}m^m r^2}{\left(m + \frac{sGP\cos\psi}{r^\alpha}\right)^m}\right.$$
$$\left. \times\ _2F_1\left(1, m; 1 - \frac{2}{\alpha}; 1 - \frac{m}{m + \frac{sGP\cos\psi}{r^\alpha}}\right)\right)\text{d}\psi. \tag{7}$$

Note that $_2F_1(\cdot, \cdot; \cdot; \cdot)$ is the hypergeometric function [12].

Proof: See Appendix A. ∎

C. Special Case: Strong Fading Environment

We consider a strong fading environment ($m = 1$), yielding Rayleigh fading. If we further assume $\alpha = 4$, much simpler single-integral representation for the coverage probability can be obtained in the following proposition.

Proposition 2 (Strong fading case): A single-integral form of the coverage probability for Rayleigh fading is given by

$$P_c = \frac{K^2}{2\pi^2}\left[\int_{\cos\frac{\pi}{K}}^1\frac{\log\left(\frac{\sqrt{1 - (\cos^2\frac{\pi}{K})z^2} + (\sin\frac{\pi}{K})z}{\sqrt{1 - (\cos^2\frac{\pi}{K})z^2} - (\sin\frac{\pi}{K})z}\right)}{\left(1 + \rho\sqrt{T}z\,\text{arcsec}\,\sqrt{1 + Tz}\right)z}\text{d}z \right.$$
$$\left. + \int_1^{\sec\frac{\pi}{K}}\frac{\log\left(\frac{\sqrt{z^2 - \cos^2\frac{\pi}{K}} + \sin\frac{\pi}{K}}{\sqrt{z^2 - \cos^2\frac{\pi}{K}} - \sin\frac{\pi}{K}}\right)}{\left(1 + \rho\sqrt{T}z\,\text{arcsec}\,\sqrt{1 + Tz}\right)z}\text{d}z\right]. \tag{8}$$

Proof: See Appendix B. ∎

If the directional beamforming without beam broadening is available, e.g., via mechanical beam steering, we obtain the upper-bounded closed-form solution for coverage probability

$$P_c^U = \frac{1}{1 + \frac{\phi_{\text{BW}}}{K}\sqrt{T}\,\text{arcsec}\,\sqrt{1 + T}}, \tag{9}$$

which can be easily calculated by substituting $\cos\theta = 1$ and $\cos\psi = 1$ and eliminating integration over them.

D. Special Case: Weak Fading Environment

We now assume each link approaches AWGN-like static channel (i.e., $m \to \infty$), which is more suitable for mmWave applications where the LOS component dominates over the NLOS multipath components [11]. Assuming large directivity gain ($G \gg 1$) and $\alpha = 4$, we obtain simple closed-form asymptotic coverage probability expression.

Proposition 3 (Weak fading case): The asymptotic coverage probability when each link experiences AWGN-like weak fading ($m \to \infty$) can be obtained as

$$\lim_{m \to \infty} P_c = \frac{8K^2 F\left(\frac{\pi}{2K}, 2\right) E\left(\frac{\pi}{2K}, 2\right)}{\pi^3 \rho \sqrt{T}}, \qquad (10)$$

where we denote that $F(\varphi, k) = \int_0^\varphi \frac{\mathrm{d}\zeta}{\sqrt{1 - k^2 \sin^2 \zeta}}$ is the elliptic integral of the first kind, and $E(\varphi, k) = \int_0^\varphi \sqrt{1 - k^2 \sin^2 \zeta}\, \mathrm{d}\zeta$ is the elliptic integral of the second kind [12].

Proof: See Appendix C. ∎

IV. Numerical Results

We provide the numerical results for the coverage probability of a typical user in a directional beamforming-based cellular network. We also provide the Monte Carlo-based simulation results for 50,000 iterations. Unless explicitly indicated, we assume the following common parameters: $\lambda = 10$, $\alpha = 4$, $P = 1$, $G = 10$dB, $K = 3$, and $\phi_{\mathrm{BW}} = 30°$.

We first show the results for Rayleigh fading. Fig. 1 depicts the coverage probability as a function of the SIR threshold for the cases with and without directional beamforming. The curve for that without directional beamforming is based on [7]. We also plot the upper-bounded coverage probability (9) for comparison. The first observation is that the coverage probability is much increased by directional beamforming, which is due to the fact that the mobile user can receive stronger beamformed desired signal while less affected by the other-cell interference caused by the neighboring cells whose beams are focused to their own mobile users. The achievable coverage probability gain is up to 10 dB. The second observation is the relative closeness between the coverage probability with directional beamforming and its upper bound considering no beam broadening effect. Although the beam broadening reduces the coverage probability, the amount of coverage loss is not significant compared with the coverage gain over the case without directional beamforming. We also observe good conformance between the analytic and simulation results.

Fig. 2 shows the coverage probability as a function of the SIR threshold for different beam widths: $\phi_{\mathrm{BW}} = 20° - 140°$. The coverage probability continuously decreases with ϕ_{BW} and finally approaches that without directional beamforming.

We now show the coverage probability results under the Nakagami-m fading model. Fig. 3 shows the coverage probability as a function of the SIR threshold for different m parameters including the special cases of $m = 1$ (Rayleigh) and $m \to \infty$ (AWGN). We can see that the coverage probability increases as m increases.

Asymptotic coverage probabilities with infinite m and large T are shown in Fig. 4. Note that the asymptotic coverage probability converges to the actual one as the SIR threshold increases, justifying our asymptotic approach.

V. Conclusion

In this paper, we analyzed the coverage probability of a cellular network when directional beamforming is employed.
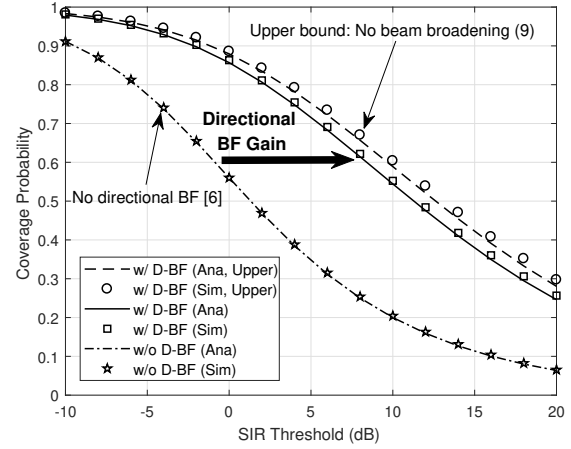
Fig. 1. Coverage probability vs. SIR threshold with and without directional beamforming. Upper-bound coverage probability is also seen for comparison.
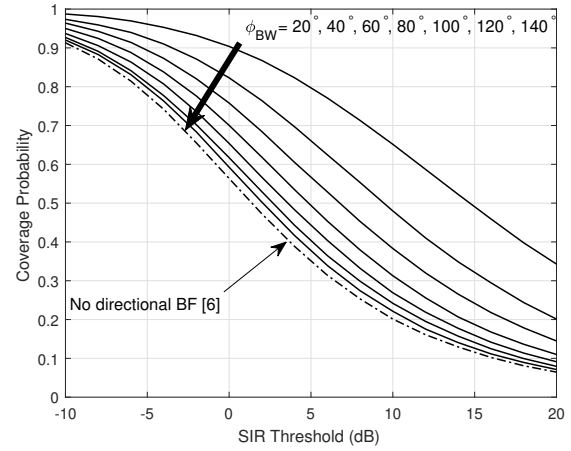
Fig. 2. Coverage probability vs. SIR threshold for different beam widths.
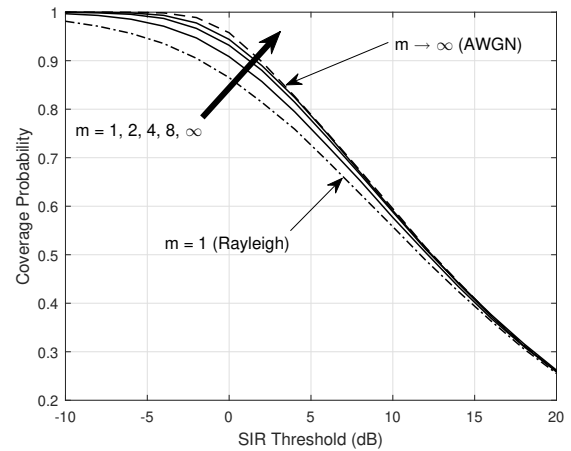
Fig. 3. Coverage probability vs. SIR threshold for different m parameters with the special cases of $m = 1$ (Rayleigh) and $m \to \infty$ (AWGN).
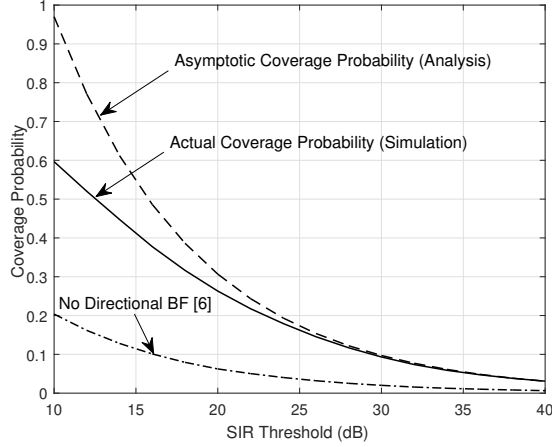
Fig. 4. Asymptotic coverage probability vs. SIR threshold when $m \to \infty$.

Analyses are done with Nakagami-m fading, NLOS-dominant Rayleigh fading ($m = 1$), and LOS-dominant static ($m \to \infty$) channels. The obtained formulae reveal that, despite some coverage loss due to the beam broadening effect, the achieved gain by directional beamforming is still significant (i.e., up to 8 dB gain in SIR).

APPENDIX A
PROOF OF PROPOSITION 1

Conditioning on r and θ with their respective PDFs $f_r(r) = 2\pi\lambda r e^{-\pi\lambda r^2}$ and $f_\theta(\theta) = K/2\pi$ [7], the coverage probability for a typical mobile user can be expressed as

$$P_c = \lambda K \int_{-\frac{\pi}{K}}^{\frac{\pi}{K}} \int_0^\infty \mathbb{P}\left(h > \frac{Tr^\alpha I_r}{GP\cos\theta}\Big|r,\theta\right) r e^{-\pi\lambda r^2} \, dr d\theta, \tag{11}$$

where

$$\mathbb{P}\left(h > \frac{Tr^\alpha I_r}{GP\cos\theta}\Big|r,\theta\right) = \mathbb{E}\left[\mathbb{P}\left(h > \frac{Tr^\alpha I_r}{GP\cos\theta}\right)\Big|r,\theta,I_r\right]$$

$$= \mathbb{E}\left[\exp\left(-\frac{mTr^\alpha I_r}{GP\cos\theta}\right)\sum_{k=0}^{m-1}\frac{1}{k!}\left(\frac{mTr^\alpha I_r}{GP\cos\theta}\right)^k\Big|r,\theta\right], \tag{12}$$

The calculation of (12) is done using the complementary cumulative distribution function (CCDF) of the Gamma distribution: $F_x^c(x) = e^{-mx}\sum_{k=0}^{m-1}\frac{(mx)^k}{k!}$.

After some mathematical manipulation and using the definition of the Laplace transform, (12) becomes

$$\mathbb{P}\left(h > \frac{Tr^\alpha I_r}{GP\cos\theta}\Big|r,\theta\right) = \sum_{k=0}^{m-1}\frac{s^k}{k!}\int_0^\infty t^k e^{-st}f_{I_r}(t)dt\Big|_{s=\frac{mTr^\alpha}{GP\cos\theta}}$$

$$= \sum_{k=0}^{m-1}\frac{(-s)^k}{k!}\frac{d^k}{ds^k}\mathcal{L}_{I_r}(s)\Big|_{s=\frac{mTr^\alpha}{GP\cos\theta}}. \tag{13}$$

Using the IID properties of g_i, l_i, and ψ_i, applying the probability generating functional (PGFL) [7] of the PPP, and

substituting the Nakagami-m PDF yields

$$\mathcal{L}_{I_r}(s) = \mathbb{E}_\psi\left[\exp\left(-\frac{2\pi\lambda_{\text{eff}}m^m}{\Gamma(m)}\int_0^\infty\int_r^\infty\frac{1-e^{-\frac{sGPg}{l^\alpha\sec\psi}}}{l^{-1}g^{1-m}e^{mg}}dldg\right)\right]$$

$$= \mathbb{E}_\psi\left[\exp\left(\pi\lambda_{\text{eff}}r^2 + \frac{2\pi\lambda_{\text{eff}}}{\alpha}\frac{m^m}{\Gamma(m)}(sGP\cos\psi g)^{\frac{2}{\alpha}}\right.$$

$$\left.\times\int_0^\infty g^{\frac{2}{\alpha}+m-1}e^{-mg}\gamma\left(-\frac{2}{\alpha},\frac{sGP\cos\psi}{r^\alpha}g\right)dg\right)\right], \tag{14}$$

where the inner integral is solved using the integration by substitution ($l^{-\alpha} = y$) and (3.381.3-4) in [12]. (14) can be further reduced with the help of (6.455.2) in [12], yielding the desired result in (7).

APPENDIX B
PROOF OF PROPOSITION 2

When $m = 1$ and $\alpha = 4$, using the Gauss' recursion functions (9.137.2) and (9.137.18) in [12], we have:

$${}_2F_1\left(1,1;\frac{1}{2};x\right) = -\frac{x{}_2F_1\left(1,1;\frac{3}{2};x\right)+{}_2F_1\left(0,1;\frac{3}{2};x\right)}{x-1}. \tag{15}$$

which can be used to simplify (7):

$$\mathcal{L}_{I_r}(s) = \frac{K}{2\pi}\int_{-\frac{\pi}{K}}^{\frac{\pi}{K}}\exp\left(-\pi\lambda_{\text{eff}}r^2\sqrt{\frac{sGP\cos\psi}{r^4}}\right.$$

$$\left.\times\text{arcsec}\sqrt{1+\frac{sGP\cos\psi}{r^4}}\right)d\psi. \tag{16}$$

Substituting (16) into (6) and integrating by substitution ($r^2 = z$) yields

$$P_c = \frac{K^2}{4\pi^2}\int_{-\frac{\pi}{K}}^{\frac{\pi}{K}}\int_{-\frac{\pi}{K}}^{\frac{\pi}{K}}\frac{1}{1+\rho\sqrt{T\frac{\cos\psi}{\cos\theta}}\,\text{arcsec}\sqrt{1+T\frac{\cos\psi}{\cos\theta}}}d\psi d\theta. \tag{17}$$

Employing a change of variable method [14], we first substitute $z = \frac{\cos\psi}{\cos\theta}$ and introduce an auxiliary variable $w = \theta$. Solving the equation $\cos\psi = z\cos w$ yields

$$\begin{aligned}\cdot\psi_1 &= \arccos(z\cos w)\\ \cdot\psi_2 &= -\arccos(z\cos w)\end{aligned} \qquad \cdot\theta_1 = w \tag{18}$$

We then derive the Jacobian

$$J(z,w) = \begin{vmatrix}\frac{\partial\psi_1}{\partial z} & \frac{\partial\psi_1}{\partial w}\\ \frac{\partial\theta_1}{\partial z} & \frac{\partial\theta_1}{\partial w}\end{vmatrix} = -\frac{\cos w}{\sqrt{1-z^2\cos^2 w}}. \tag{19}$$

The derived joint PDF of z and w is given by

$$f_{z,w}(z,w) = \frac{K^2}{2\pi^2}\frac{\cos w}{\sqrt{1-z^2\cos^2 w}}, \tag{20}$$

for $\cos\frac{\pi}{K}\le z < 1$ and $-\frac{\pi}{K}\le w < \frac{\pi}{K}$.
Marginalizing over w using (2.597.5) in [12] yields

$$f_z(z) = \frac{K^2}{2\pi^2\sqrt{1-z^2}}\int_{-\frac{\pi}{K}}^{\frac{\pi}{K}}\frac{\cos w}{\sqrt{1+\frac{z^2}{1-z^2}\cos^2 w}}dw$$

$$= \frac{K^2}{2\pi^2 z}\left[\log\left(\frac{\sqrt{1-(\cos^2\frac{\pi}{K})z^2}+(\sin\frac{\pi}{K})z}{\sqrt{1-(\cos^2\frac{\pi}{K})z^2}-(\sin\frac{\pi}{K})z}\right)\right], \tag{21}$$

for $\cos\frac{\pi}{K} \le z < 1$.

Now we set $w = \psi$ in order to find the PDF of z for the range of $1 \le z < \sec\frac{\pi}{K}$. Solving $\cos\theta = \frac{\cos w}{z}$ yields

$$
\begin{aligned}
&\cdot\,\theta_1 = \arccos\left(\frac{\cos w}{z}\right) \\
&\cdot\,\theta_2 = -\arccos\left(\frac{\cos w}{z}\right)
\end{aligned}
\qquad \cdot\,\psi_1 = w. \tag{22}
$$

Similar approach to the above $\cos\frac{\pi}{K} \le z < 1$ case (i.e., Jacobian calculation and marginalization on w) yields the PDF of z for the range of $1 \le z < \sec\frac{\pi}{K}$, as follows:

$$
f_z(z) = \frac{K^2}{2\pi^2 z}\left[\log\left(\frac{\sqrt{z^2 - \cos^2\frac{\pi}{K}} + \sin\frac{\pi}{K}}{\sqrt{z^2 - \cos^2\frac{\pi}{K}} - \sin\frac{\pi}{K}}\right)\right]. \tag{23}
$$

Replacing z and $f_z(z)$ into (17), integrating it yields (8).

APPENDIX C
PROOF OF PROPOSITION 3

Assuming $m \to \infty$, the Laplace transform $\mathcal{L}_{I_r}(s)$ under the Nakagami-m fading in (7) can be simplified to

$$
\mathcal{L}_{I_r}(s) = \frac{e^{\pi\lambda_{\text{eff}}r^2}}{2\pi/K}\int_{-\frac{\pi}{K}}^{\frac{\pi}{K}}\exp\left(\frac{(sGP\cos\psi)^{\frac{2}{\alpha}}}{\alpha/2\pi\lambda_{\text{eff}}}\gamma\left(-\frac{2}{\alpha}, \frac{sGP\cos\psi}{r^\alpha}\right)\right)d\psi, \tag{24}
$$

where $\gamma(a,x) = \int_0^x e^{-t}t^{a-1}dt$ is the lower incomplete Gamma function [12]. Since we employ a high directivity gain, i.e., $G \gg 1$, the incomplete gamma function in (24) becomes

$$
\gamma\left(-\frac{2}{\alpha}, \frac{sGP\cos\psi}{r^\alpha}\right) \to \Gamma\left(-\frac{2}{\alpha}\right). \tag{25}
$$

Using (25) and assuming $\alpha = 4$, (24) is reexpressed as

$$
\mathcal{L}_{I_r}(s) = \frac{K}{2\pi}e^{\pi\lambda_{\text{eff}}r^2}\int_{-\frac{\pi}{K}}^{\frac{\pi}{K}}\exp\left(-\pi^{\frac{3}{2}}\lambda_{\text{eff}}\sqrt{sGP\cos\psi}\right)d\psi, \tag{26}
$$

Using (0.433.1) of [12], the k-th derivative of $\mathcal{L}_{I_r}(s)$ is

$$
\frac{d^k}{ds^k}\mathcal{L}_{I_r}(s) = \frac{K}{2\pi}e^{\pi\lambda_{\text{eff}}r^2}\int_{-\frac{\pi}{K}}^{\frac{\pi}{K}}\sum_{p=0}^{k-1}\frac{(-1)^p(k+p-1)!}{p!(k-p-1)!}
$$

$$
\times\left(-\pi^{\frac{3}{2}}\lambda_{\text{eff}}\sqrt{GP\cos\psi}\right)^{k-p}\frac{\exp\left(-\pi^{\frac{3}{2}}\lambda_{\text{eff}}\sqrt{sGP\cos\psi}\right)}{\left(2\sqrt{s}\right)^{k+p}}d\psi. \tag{27}
$$

Substituting (27) into the general coverage expression (6), integrating it over r, and using (15.4.1) of [15] yields

$$
P_c = \frac{\lambda K^2}{4\pi^2}\int_{-\frac{\pi}{K}}^{\frac{\pi}{K}}\int_{-\frac{\pi}{K}}^{\frac{\pi}{K}}\frac{1}{\lambda - \lambda_{\text{eff}}\left(1 - \sqrt{\frac{\pi mT\cos\psi}{\cos\theta}}\right)}\left[\frac{2\delta(\theta,\psi)(1+\delta(\theta,\psi))}{2+\delta(\theta,\psi)}\right.
$$

$$
\times\left(1 - \left(\frac{-1}{\delta(\theta,\psi)(2+\delta(\theta,\psi))}\right)^m\right) - 2\delta(\theta,\psi)\sum_{k=0}^{m-1}\frac{(2k)!}{k!(k+1)!}
$$

$$
\left.\times\left(\frac{1}{4+2\delta(\theta,\psi)}\right)^{k+1}{}_2F_1\left(1-k, k; k+2; -\frac{\delta(\theta,\psi)}{2}\right)\right]d\theta d\psi, \tag{28}
$$

where

$$
\delta(\theta,\psi) = -\left(1 + \frac{\lambda - \lambda_{\text{eff}}}{\lambda_{\text{eff}}\sqrt{\frac{\pi mT\cos\psi}{\cos\theta}}}\right). \tag{29}
$$

Since ${}_2F_1(1-k, k; k+2; x)$ in (28) is continuous at $x = \frac{1}{2}$, the following limiting property holds:

$$
\lim_{m\to\infty}{}_2F_1\left(1-k, k; k+2; -\frac{\delta(\theta,\psi)}{2}\right) = {}_2F_1\left(1-k, k; k+2; \frac{1}{2}\right)
$$

$$
= 2^{-k}(k+1), \tag{30}
$$

where

$$
\lim_{m\to\infty}\delta(\theta,\psi) = -1. \tag{31}
$$

Using the algebraic limit theorem and substituting (30) and (31) into (28), we obtain the following asymptotic coverage probability:

$$
\lim_{m\to\infty}P_c = \frac{\lambda K^2}{4\pi^2}\int_{-\frac{\pi}{K}}^{\frac{\pi}{K}}\int_{-\frac{\pi}{K}}^{\frac{\pi}{K}}\lim_{m\to\infty}\frac{m2^{1-2m}\binom{2m}{m}}{\lambda - \lambda_{\text{eff}}\left(1 - \sqrt{\frac{\pi mT\cos\psi}{\cos\theta}}\right)}d\theta d\psi
$$

$$
= \frac{\lambda K^2}{2\pi^3\lambda_{\text{eff}}\sqrt{T}}\int_{-\frac{\pi}{K}}^{\frac{\pi}{K}}\int_{-\frac{\pi}{K}}^{\frac{\pi}{K}}\sqrt{\frac{\cos\theta}{\cos\psi}}d\theta d\psi, \tag{32}
$$

where the limit can be easily obtained by applying Sterling's approximation [15]. The double integral can be solved using (2.571.4) and (2.576.1) in [12], yielding the desired result (10).

REFERENCES

[1] J. G. Andrews *et al.*, "What will 5G be?" *IEEE J. Sel. Areas Commun.*, vol. 32, no. 6, pp. 1065–1082, Jun. 2014.

[2] W. Roh *et al.*, "Millimeter-wave beamforming as an enabling technology for 5G cellular communications: Theoretical feasibility and prototype results," *IEEE Commun. Mag.*, vol. 52, no. 2, pp. 106–113, Feb. 2014.

[3] W. H. Kummer, "Basic array theory," *Proc. IEEE*, vol. 80, no. 1, pp. 127–140, Jan. 1992.

[4] A. Elshafiy and A. Sampath, "Beam broadening for 5G millimeter wave systems," in *Proc. IEEE Wireless Commun. Netw. Conf. (WCNC 2019)*, Apr. 2019.

[5] H. J. Visser, *Array and Phased Array Antenna Basics*. John Wiley & Sons, 2005.

[6] W. H. Chin, Z. Fan, and R. Haines, "Emerging technologies and research challenges for 5G wireless networks," *IEEE Wireless Commun. Mag.*, vol. 21, no. 2, pp. 106–112, Apr. 2014.

[7] J. G. Andrews, F. Baccelli, and R. K. Ganti, "A tractable approach to coverage and rate in cellular networks," *IEEE Trans. Commun.*, vol. 59, no. 11, pp. 3122–3134, Nov. 2011.

[8] J. G. Andrews, T. Bai, M. N. Kulkarni, A. Alkhateeb, A. K. Gupta, and R. W. Heath, "Modeling and analyzing millimeter wave cellular systems," *IEEE Trans. Commun.*, vol. 65, no. 1, pp. 403–430, Jan. 2017.

[9] 3GPP TR 38.900, "Channel model for frequency spectrum above 6 GHz," v. 1.0.1, Jun. 2016.

[10] A. Ghasemi and E. S. Sousa, "Fundamental limits of spectrum-sharing in fading environments," *IEEE Trans. Wireless Commun.*, vol. 6, no. 2, pp. 649–658, Feb. 2007.

[11] T. Bai and R. W. Heath, "Coverage and rate analysis for millimeter-wave cellular networks," *IEEE Trans. Wireless Commun.*, vol. 14, no. 2, pp. 1100–1114, Feb. 2015.

[12] I. S. Gradshteyn and I. M. Ryzhik, *Tables of Integrals, Series, and Products*, 7th ed. London, UK: Academic Press, 2007.

[13] A. Thornburg, T. Bai, and R. W. Heath, "Performance analysis of outdoor mmWave ad hoc networks," *IEEE Trans. Signal Process.*, vol. 64, no. 15, pp. 4065–4079, Aug. 2016.

[14] A. Papoulis and S. U. Pillai, *Probability, Random Variables and Stochastic Processes*, 4th ed. McGraw-Hill, 2002.

[15] M. Abramowitz and I. A. Stegun, *Handbook of Mathematical Functions With Formulas, Graphs, and Mathematical Tables*, ser. National Bureau of Standards Applied Mathematics. U.S. Gvnt. Printing Office, 1964.